

Full counting statistics of interacting lattice gases after an expansion: quantifying many-body coherence from atom correlations

Gaétan Hercé,^{1,*} Jan-Philipp Bureik,^{1,*} Antoine Ténart,¹ Alain Aspect,¹ Alexandre Dareaux,¹ and David Clément¹

¹*Université Paris-Saclay, Institut d'Optique Graduate School, CNRS, Laboratoire Charles Fabry, 91127, Palaiseau, France*

(Dated: July 29, 2022)

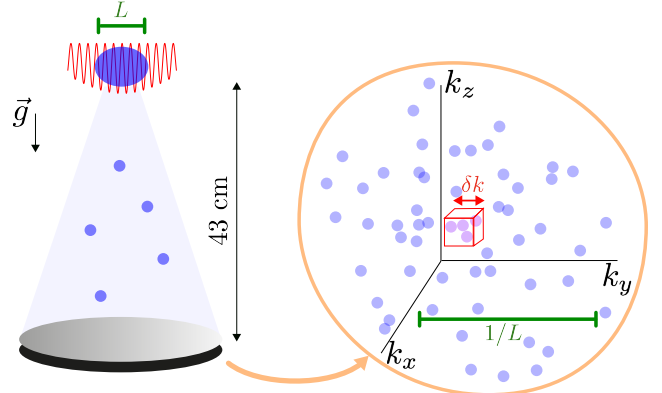
We study the full counting statistics (FCS) of quantum gases in samples of thousands of interacting bosons, detected atom-by-atom after a long free-fall expansion. In this far-field configuration, the FCS reveals the many-body coherence from which we characterize iconic states of interacting lattice bosons, by deducing the normalized correlations $g^{(n)}(0)$ up to the order $n = 6$. In Mott insulators, we find a thermal FCS characterized by perfectly-contrasted correlations $g^{(n)}(0) = n!$. In interacting Bose superfluids, we observe small deviations to the Poisson FCS and to the ideal values $g^{(n)}(0) = 1$ expected for a pure condensate. To describe these deviations, we introduce a heuristic model that includes an incoherent contribution attributed to the depletion of the condensate. The predictions of the model agree quantitatively with our measurements over a large range of interaction strengths, suggesting that the condensate component exhibits a full coherence $g^{(n)}(0) = 1$ at any order n up to $n = 6$. The approach demonstrated here is readily extendable to characterize a large variety of interacting quantum states and phase transitions.

I. INTRODUCTION

The dispersion of a physical quantity contains important information, beyond that obtained from its average value. The analysis of quantum and thermal noise is central in various systems, ranging from quantum electronics [1] and quantum optics [2] to quantum gases [3–5]. The ultimate precision on the measurement of noise is given by the full counting statistics (FCS) [6], which is obtained with single-particle-resolved detection methods that provide the number of particles detected in a given time and/or space interval. These methods yield high-order moments of the particle number, beyond the variance. Probing high-order moments is a means to study quantum phase transitions [7–9], universality [10, 11], entanglement properties [12] or out-of-equilibrium dynamics [13]. The FCS has indeed successfully characterized various phenomena in mesoscopic conductors [1, 6, 14, 15], Rydberg [16–18] and non-interacting [19, 20] atomic gases.

From a Quantum Information perspective, the FCS holds great promises for large ensembles of particles. In contrast to a full-state tomography [21], the FCS is accessible even in large systems as it probes information only about the diagonal part of the n -body density matrices (*i.e.* populations). Although it does not contain the total information about the quantum system, the FCS is sufficient to identify many (but not all) quantum states without resorting to a consuming tomography. A similar idea was introduced by R. Glauber to characterize light sources from photon correlations at any order [22]. For Gaussian states, for which the Wigner function is positive [2], measuring the FCS or the magnitudes of correlation functions is indeed equivalent. Moreover, recent

works have shown that applying random unitary transformations before measuring the FCS provides access to non-diagonal correlators [23, 24], further motivating the development of experimental approaches to the FCS, in particular in interacting systems.



Single-atom detector

FIG. 1. **(Left)** Free-fall expansion of interacting quantum gases of metastable Helium-4 from a three-dimensional optical lattice. **(Right)** Sketch of the 3D positions of individual atoms detected after an expansion. The full counting statistics $P(N_\Omega)$ describes the statistics of the atom number N_Ω detected in a small voxel of volume $V_\Omega \sim (\delta k)^3$ (red cube). To reveal the many-body coherence properties of the trapped gas of size L , δk is chosen inferior to $1/L$, $\delta k \times L \ll 1$.

In this letter, we report the measurement of the full counting statistics in large three-dimensional (3D) ensembles ($\sim 5 \times 10^3$ atoms) of interacting lattice bosons after a free-fall expansion (see Fig. 1). This configuration is analogous to the far-field regime of light propagation during which interferences take place, and after which the FCS identifies quantum states through their many-body coherence [25]. In quantum gases, far-field – or momen-

* These authors contributed equally to this work.

tum – correlations have been measured with single-atom detection in non-interacting and non-degenerate bosonic [26, 27] and fermionic [28, 29] gases and in Bose-Einstein condensates [30]. More recently interacting lattice bosons [31–33] and interacting fermions [34] were probed. However, the FCS and high-order correlations have thus far been measured only in 1D thermal gases of non-interacting bosons [27]. Here, we study various regimes of interacting 3D Bose gases across the superfluid-to-Mott phase transition, from weakly-interacting Bose superfluids to Mott insulators.

We characterize the FCS by measuring the probability distribution of the atom number N_Ω falling in a small voxel V_Ω (see Fig. 1) and we determine the magnitudes $g^{(n)}(0)$ of correlation functions (up to $n = 6$) based on the factorial moments of N_Ω . We compare our findings to the many-body coherence properties expected for pure state descriptions of both the superfluid and the Mott phase. Although we find an almost exact agreement, we observe small deviations to the predictions for a pure condensate in the case of Bose superfluids. Since, to our knowledge, ab-initio calculations of the measured quantities with thousands of interacting atoms are beyond state-of-the-art numerics, we introduce a heuristic model that includes the contribution of the condensate depletion. Its predictions are in quantitative agreement with our observations, which leads us to conclude that the condensate component exhibits a full coherence, $g^{(n)}(0) = 1$ at least up to $n = 6$.

II. FULL COUNTING STATISTICS (FCS) OF PURE-STATE BECS AND MOTT INSULATORS

Textbook descriptions of Bose-Einstein Condensates (BECs) and Mott insulators are based on pure states. Bose-Einstein condensation is associated with the breaking of phase symmetry [35] whose complex order parameter defines a coherent state describing the BEC. In a grand canonical approach, coherent states have a Poisson counting statistics, $P(N_\Omega) = \langle N_\Omega \rangle^{N_\Omega} \exp[-\langle N_\Omega \rangle]/N_\Omega!$ where N_Ω is the number of detected bosons in the considered volume V_Ω , and a full coherence $g^{(n)} = 1$ at any order n of normalized correlations either in position or in momentum space [22]. In our experiment, we determine $g^{(n)}(0) = g^{(n)}(\mathbf{k}, \mathbf{k}, \dots, \mathbf{k})$, where \mathbf{k} is the momentum at which correlations are evaluated, *i.e.* where the volume V_Ω is located, and for a pure coherent state we expect $g^{(n)}(0) = 1$ at all orders. In contrast, a “perfect” Mott insulator – a uniform Mott insulator at zero temperature – is thought of as a Fock state in the (in-trap) position basis. In the momentum basis, which is probed after a long expansion from the trap, it is expected to exhibit thermal statistics [31, 36, 37]. This is because far-field correlations reflect multi-particle interferences from a discrete series of emitters (atoms in the lattice sites) with no coherence between the sites (no tunnelling), a situation analog to that of a thermal state without site-

to-site phase coherence. Thermal states are characterized by a counting statistics $P(N_\Omega) = (1 - q)q^{N_\Omega}$ where $q = \langle N_\Omega \rangle / (1 + \langle N_\Omega \rangle)$ and $g^{(n)}(\mathbf{k}, \mathbf{k}, \dots, \mathbf{k}) = n!$ [38]. Note that both the Poisson and the thermal FCS are fully determined by a single parameter, the average number of particles $\langle N_\Omega \rangle$, as a result of the Gaussian character of their quantum state [2]. For Gaussian states, a detection efficiency η smaller than one does not affect the measurement of the FCS – nor that of $g^{(n)}$ – which is of practical interest since $\eta < 1$ in experiments.

Whether these many-body coherence properties associated to pure states describe the outcome of experiments is not granted. On the one hand, pure states are only approximated descriptions of states produced in an experiment because of the coupling to the environment. Determining the level – *e.g.* the order n of correlations – up to which a description in terms of pure states is valid provides a quantitative certification of experimental realizations. In the context of the development of platforms for quantum technologies, such a certification is certainly of interest. On the other hand, the properties of quantum states produced at thermodynamical equilibrium are affected by constraints on macroscopic quantities. In the canonical (or micro-canonical) ensemble there are no fluctuations of the *total* BEC atom number N_{BEC} in a gas of non-interacting bosons at zero temperature [39]: N_{BEC} is fixed to the total atom number, $N_{\text{BEC}} = N$. The statistics of N_{BEC} is therefore not that of a coherent state [40]. To alleviate such global constraints and mimic a grand canonical ensemble, one may probe the FCS within a volume V_Ω much smaller than that, V_{BEC} , occupied by the BEC. The volume $V_{\text{BEC}} - V_\Omega \sim V_{\text{BEC}}$ then serves as a reservoir for the sub-volume V_Ω where the number of bosons $N_\Omega \ll N$ may fluctuate [41].

Measuring the FCS in small sub-volumes V_Ω is also crucial if correlation functions $g^{(n)}(\mathbf{k}, \mathbf{k}', \dots, \mathbf{k}'')$ are bell shaped with widths $l_c^{(n)}$. While this is not an issue for a coherent state which is fully coherent over the entire volume it occupies, the statistics of a thermal state must be probed over an elementary cell of the phase space. This is well known in the case of the Hanbury-Brown and Twiss effect where the property $g^{(2)}(\mathbf{k}, \mathbf{k}') = 2$ is expected only if $|\mathbf{k} - \mathbf{k}'|$ is less than the width of the far-field diffraction pattern associated with the source size. Here, it means that fully-contrasted correlations are expected only when computed in a volume smaller than $V_c^{(n)} = [l_c^{(n)}]^3$ since particles distant by $l_c^{(n)}$ are essentially uncorrelated. In the far-field, the correlation lengths of Mott insulators and of thermal Bose gases are set by the inverse in-trap size, $l_c^{(n)} \sim 1/L$ [31, 32]. As a result, observing fully-contrasted FCS and n -body correlations requires using $V_\Omega \ll 1/L^3$. This condition also ensures the above-mentioned criterion on probing BECs as the volume occupied by the BEC in the momentum space is set by $\Delta k \sim 1.6/L$ [42]. With these considerations in mind, in the following we compute the counting statistics in a volume $V_\Omega \sim (\delta k)^3$ of the momentum space such that $\delta k \times L \ll 1$, where L is the in-trap size of the gas

(see Fig. 1). As illustrated below, this choice is essential to correctly reveal the full statistical properties.

III. MEASUREMENT OF THE FCS IN MOTT INSULATORS AND BOSE SUPERFLUIDS

Our measurement of the FCS in the far-field exploits 3D atom-by-atom detection of metastable Helium-4 ($^4\text{He}^*$) after a long free-fall expansion [43, 44], with a detection efficiency of $\eta = 0.53(2)$ per atom and negligible dark counts (see Fig. 1). For an individual run, we register the number of atoms in each of the voxels V_Ω mentioned above, and we use more than 2000 runs to obtain the probability distribution in each voxel. We apply this approach to probe equilibrium quantum states of $^4\text{He}^*$ atoms loaded in the lowest energy-band of a three-dimensional (3D) optical lattice [45]. The lattice implements the 3D Bose-Hubbard Hamiltonian whose main parameters are the tunnelling amplitude J and the on-site (repulsive) interaction U .

We first investigate the thermal nature of Mott insulators in the momentum space. We realize Mott insulators with $N = 10(3) \times 10^3$ atoms at $U/J = 95$, which corresponds to a lattice filling of one atom per site at the trap center [31] and an almost uniform filling of the first Brillouin zone in the momentum space. To compute the counting statistics in this first set of experiments, we divide the first Brillouin zone into cubic voxels V_Ω of size $\delta k = 4 \times 10^{-2} k_d \ll 1/L$ and average the probability distributions measured over all these voxels. Here $k_d = 2\pi/d$ is the momentum associated with the lattice spacing $d = 775$ nm. The resulting FCS of the Mott state is shown in Fig. 2(a). It is found to be in excellent agreement with a thermal statistics whose average atom number is that measured in the experiment, $\langle N_\Omega \rangle = 0.46(5)$.

The statistical properties of the Mott state are also revealed through the magnitudes $g^{(n)}(0)$ of the normalized correlation functions, as an alternative to the probability distribution $P(N_\Omega)$. We determine $g^{(n)}(0)$ from the factorial moments of the detected atom number, transposing a well-known approach in quantum optics [46]. The correlation functions of quantum optics [22] are defined with normal ordering of the destruction operators, since a detected photon is destroyed and there is one photon less in the volume of measurement. Even if it is not always emphasized, the correlation functions in quantum optics are indeed calculated from the factorial moments, and it is remarkable that the corresponding quantities in classical statistics are also based on factorial moments [47]. In the experiments reported here, each detected He^* atom is destroyed and the results of quantum optics can be directly transposed. Finally, we use a similar approach as that used for $P(N_\Omega)$ – averaging over many runs and then over many voxels within the first Brillouin zone.

We first evaluate the factorial moments of the atom number $N_{\delta k_\perp}$ detected in voxels of adjustable volume $V(\delta k_\perp) = \delta k \delta k_\perp^2$ and normalize them with the average

atom number in the same voxels, to obtain

$$g_{\delta k_\perp}^{(n)}(0) = \frac{\sum_j \langle N_{\delta k_\perp} (N_{\delta k_\perp} - 1) \dots (N_{\delta k_\perp} - n + 1) \rangle_j}{\sum_j \langle N_{\delta k_\perp} \rangle_j^n} \quad (1)$$

where \sum_j refers to the sum over all the voxels (labelled by the index j) belonging to the first Brillouin zone. The magnitudes $g^{(n)}(0)$ of the n -body correlation functions are obtained from extrapolating $g_{\delta k_\perp}^{(n)}(0)$ at $\delta k_\perp \rightarrow \delta k$ (see Appendix A). The results are plotted in Fig. 2(c), along with the prediction for thermal states, $g^{(n)}(0) = n!$. The excellent quantitative agreement demonstrates that the n -body coherence of a unity-filling Mott insulator is thermal [31, 36, 37]. The momentum-space FCS of a Mott insulator is thus identical to that of a statistical mixture of thermal bosons. Their full correlation functions however differ in their sizes $l_c^{(n)}$ which are determined by their different in-trap sizes and the incompressible (*resp.* compressible) character of Mott insulators (*resp.* thermal gases) [31].

In a second set of experiments, we address the n -body coherence of the BEC component in lattice superfluids with $N = 5(1) \times 10^3$ at $U/J = 5$. In the momentum space, the BEC occupies a volume of width $\Delta k \simeq 0.15 k_d$ centered at $\mathbf{k} = \mathbf{0}$ [33]. This volume contains many atoms in each run and the statistics of the atom number falling in a sphere S_Ω of a radius $\delta k = 0.025 k_d \ll \Delta k$, centered at $\mathbf{k} = \mathbf{0}$, is sufficient to extract the counting statistics. We measure the counting statistics $P(N_\Omega)$ in S_Ω over about 2000 experimental runs, with the results plotted in Fig. 2(b). It is compared with Poisson and thermal statistics whose average atom number $\langle N_\Omega \rangle = 5.3(2)$ is that measured in the experiment. The counting statistics in the BEC mode is close to the Poisson FCS and clearly differs from the thermal FCS. This is confirmed by the measured values of $g^{(n)}(0)$ calculated from the normalized factorial moments of N_Ω ,

$$g^{(n)}(0) = \frac{\langle N_\Omega (N_\Omega - 1) \dots (N_\Omega - n + 1) \rangle}{\langle N_\Omega \rangle^n} \quad (2)$$

In Fig. 2c we plot $g^{(n)}(0)$ as a function of n and find that $g^{(n)}(0) \sim 1$ at any order n in the BEC mode. These results, predicted by Glauber for a fully coherent sample, are in striking contrast with those of the Mott state, a difference that illustrates the outstanding capabilities of the FCS measured after an expansion to reveal the n -body coherence.

Surprisingly, however, our measurements in the BEC mode deviate from the predictions for a coherent state and from a previous observation [30]: the deviation in the FCS (see Fig. 2(b)) is reflected in the fact that $g^{(n)}(0) > 1$, as shown in Fig. 2(d). To verify that the observed deviations are statistically meaningful, we apply our computation of the n -body correlations to a randomized set, with the same numbers of atoms and of runs. This randomized set is obtained by randomly shuffling

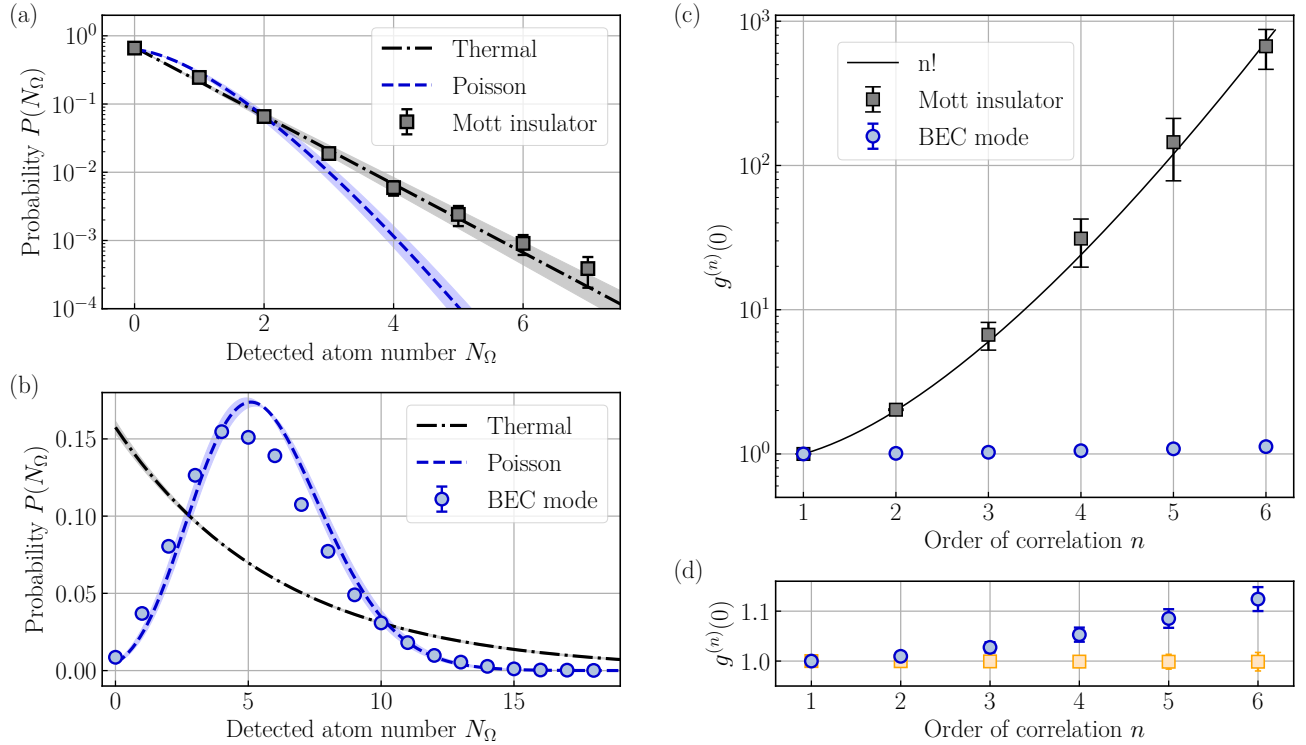


FIG. 2. **(a)** Full Counting statistics $P(N_\Omega)$ to find N_Ω atoms in a small volume V_Ω of the momentum space when probing a Mott insulator with unity filling (black circles). The predictions for thermal (*resp.* Poissonian) statistics is shown as a dashed-dotted black (*resp.* dashed blue) line. We use the measured value $\langle N_\Omega \rangle = 0.46(5)$ for the theoretical predictions (the shaded areas reflect the uncertainty on $\langle N_\Omega \rangle$). The error bars denote the statistical uncertainty (standard deviation) estimated with the bootstrapping method. **(b)** Same as (a) in the BEC mode ($\mathbf{k} = \mathbf{0}$) of interacting lattice superfluids (SF) with $U/J = 5$. The mean atom number is $\langle N_\Omega \rangle = 5.3(2)$. Error bars are smaller than the dots. **(c)** Magnitude $g^{(n)}(\mathbf{0})$ of n -body correlations plotted as a function of the order n of the correlations. The black squares correspond to a Mott insulator (panel a) and the blue circles to a Bose superfluid (panel b). The prediction for thermal Gaussian states, $g^{(n)}(0) = n!$, is shown as a black solid line. **(d)** $g^{(n)}(\mathbf{0})$ in the SF (blue circles, same data as in (c)) and in the randomized set (orange squares).

the detected atoms across the experimental runs. Doing so, atom correlations present within individual runs (*i.e.* before shuffling) should vanish, and a Poisson statistics should be observed as a result of the discrete nature of our detection method applied to fully independent events. Indeed we find $g^{(n)}(0) = 1.00(2)$ at any order n of the randomized ensemble (see the orange squares in Fig. 2(d)), confirming that the deviations in the (non-randomised) experimental data are significant. Note that the randomization method also yields a Poisson statistics when applied to the Mott insulator data set. In the next section, we propose an interpretation of the tiny deviations $g^{(n)}(0) > 1$ revealed by our experiment in the case of lattice superfluids.

IV. COHERENT FRACTION OF BOSE SUPERFLUIDS IN THE BEC MODE

A Poisson statistics is expected when only atoms from the BEC, which is thought of as a coherent state, contribute to the measured statistics in a volume S_Ω that is

small compared to the coherence volume. At a macroscopic level though, a fraction of the total atom number is expelled from the BEC by the finite interactions (quantum depletion) and by the finite temperature (thermal depletion). Even if it amounts to a negligible fraction of the atom number N_Ω falling in S_Ω , the total depletion of the condensate may contribute to the measured statistics. Building on these considerations, we introduce a heuristic model that assumes (*i*) that atoms in the BEC and in the depletion contribute independently to the measured counting statistics in S_Ω [40], and (*ii*) that the BEC is a coherent state while the depletion exhibits thermal statistics in S_Ω . We define the “coherent fraction” f_{coh} as the fraction of the BEC atoms falling within S_Ω . We emphasize that describing the contribution of the quantum depletion in S_Ω with a thermal statistics is an assumption. We have shown that the statistics of the quantum depletion is thermal when measured at *non-zero* momenta, outside the BEC [32]. However, whether this is also valid for small momenta belonging to the BEC mode is difficult to assess in a harmonic trap. In contrast to homogeneous systems for which the momentum

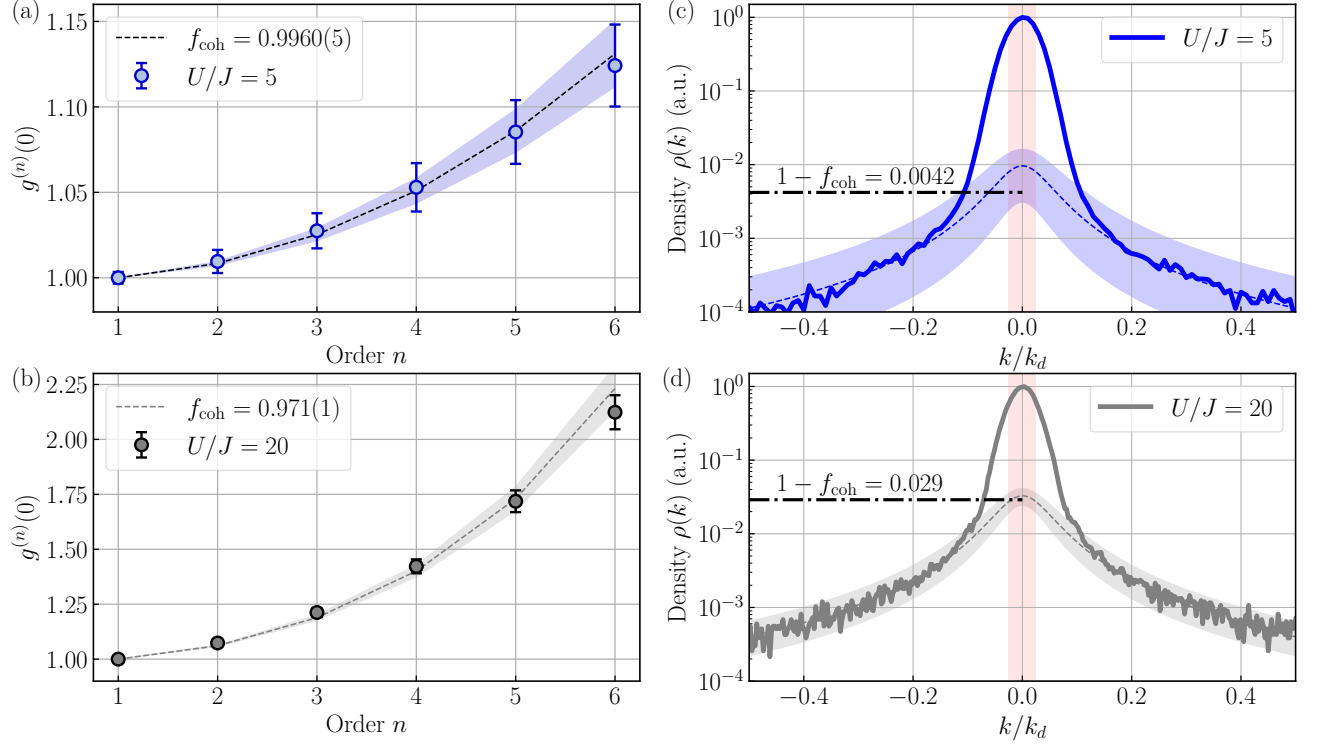


FIG. 3. (a)-(b) Plots of $g^{(n)}(0)$ measured at $\mathbf{k} = \mathbf{0}$ in lattice superfluids with $U/J = 5$ and $U/J = 20$. The data in panel (a) is identical to that of shown in Fig. 2(c). The dashed lines (*resp.* the shaded areas) are the predictions of the model with the values f_{coh} (*resp.* the uncertainties on f_{coh}) fitted to the data. (c)-(d) Plots of 1D cuts through the momentum densities measured at $U/J = 5$ and $U/J = 20$ and normalized to their value at $k = 0$. The vertical shaded area indicates the volume occupied by the sphere S_Ω where the counting statistics is evaluated. The horizontal dashed-dotted lines indicate the fitted values $1 - f_{\text{coh}}$. The dashed lines are Lorentzian functions fitted to the tails of the densities in the range $[0.2k_d, 0.5k_d]$ in order to estimate the density of the depletion at $k = 0$ (the shaded areas represent the error from the fitted parameters).

is a good quantum number, in the harmonically-trapped case the quantum depletion contributes to the FCS measured at $\mathbf{k} = \mathbf{0}$. This contribution is non-trivial since the ground-state of weakly-interacting bosons is a coherent superposition of the BEC and the quantum depletion.

With the hypotheses of our model, we obtain an analytical prediction for $g^{(n)}(0)$ that depends only on the coherent fraction f_{coh} (see Appendix C),

$$g^{(n)}(0) - 1 = \sum_{p=1}^{n-1} \left[(n-p)! \binom{n}{p}^2 - \binom{n}{p} \right] f_{\text{coh}}^p (1-f_{\text{coh}})^{n-p} \quad (3)$$

In Fig. 3(a), we fit the experimental data shown in Fig. 2(d) with the analytical prediction of Eq. (3), finding a good agreement with the coherent fraction as the only adjustable parameter (found equal to $f_c = 0.9960(5)$ for the case of $U/J = 5$). We then repeated our measurements for various condensate fractions. To do so, we change the lattice depth to obtain ratios of on-site interaction U to tunnelling amplitude J ranging from $U/J = 2$ to $U/J = 22$. In this range of parameters, the gas remains far from entering the Mott insulator regime expected at the critical ratio $(U/J)_c \simeq 25 - 30$ [45].

In Fig. 3(b) we plot the magnitude of the n -body correlations for a lattice superfluids with an increased interaction $U/J = 20$. The deviation from the ideal coherent state is increased, in qualitative agreement with the physical picture at the root of the model. To be quantitative, we fit the experimental data with the analytical prediction of Eq. (3), see Fig. 3. Firstly, we confirm that Eq. (3) correctly fits the values of $g^{(n)}(0)$ with a single adjustable parameter f_{coh} . Secondly, the extracted values of f_{coh} decrease with the interaction strength as intuitively expected. The uncertainty on the values f_{coh} is small, at the $\sim 0.1\%$ level. As can be inferred from Fig. 3(a)-(b), the larger the order n of correlations we measure, the smaller the uncertainty on f_{coh} . This illustrates the extreme sensitivity of high-order correlations to probe many-body coherence.

A quantitative test of the model would compare the value $1 - f_{\text{coh}}$ to the fraction η_D of depleted atoms detected within S_{BEC} . We are not aware of a quantitative analytical prediction for η_D in 3D interacting trapped lattice Bose gases. However, an indirect comparison is amenable from measuring the momentum densities. In Fig 3(c)-(d), we plot 1D cuts through the momentum densities measured at $U/J = 5$ and $U/J = 20$ and we fit

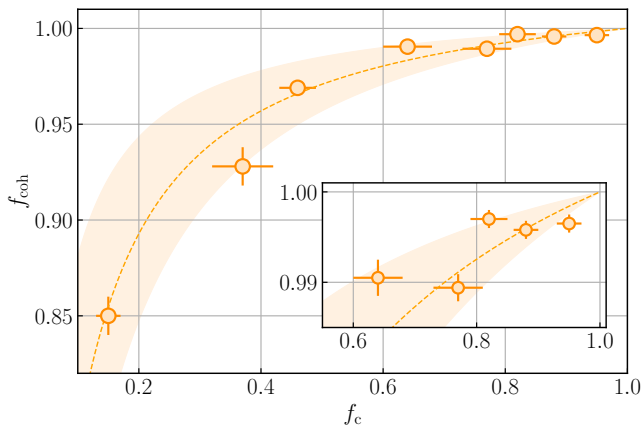


FIG. 4. Coherent fraction f_{coh} as a function of the condensate fraction f_c . The dashed-line is the prediction of Eq. (4) where the ratio $\mathcal{V}_c/\mathcal{V}_d = 0.03(1)$ is evaluated from the measured density profiles (see Appendix D). The shaded area reflects the uncertainty on $\mathcal{V}_c/\mathcal{V}_d$.

the tails (in the range $[0.2k_d, 0.5k_d]$) with a Lorentzian function to extrapolate the density of the depletion at $k = 0$. Note that using a Lorentzian function is an arbitrary choice which happens to correctly fit the tails. This analysis indicates that the values $1 - f_{\text{coh}}$ are compatible with the extrapolated densities, while both quantities vary by one order of magnitude.

To further assess the validity of the model, we proceed with a quantitative comparison of the measured coherent fraction to the measured condensate fraction [43]. The coherent fraction f_{coh} in S_Ω differs from the condensate fraction f_c of the entire gas since the radius of S_Ω is much smaller than $1/L$. Moreover, the scaling of f_{coh} with f_c is non-linear since f_{coh} reveals the BEC atom number in a small volume S_Ω where the BEC contribution is maximum while that of the depletion is small (except when $f_c \ll 1$). The volumes occupied by the BEC (\mathcal{V}_c) and by the depletion (\mathcal{V}_d) set their respective contributions. A simple estimate (see Appendix D) leads to

$$f_{\text{coh}} \simeq \frac{f_c}{f_c + (1 - f_c)\mathcal{V}_c/\mathcal{V}_d}. \quad (4)$$

In Fig. 4 we plot the measured values of f_{coh} and f_c , along with the prediction of Eq. (4). Here, f_c is obtained similarly to [43] and the ratio $\mathcal{V}_c/\mathcal{V}_d$ used to plot Eq. (4) is estimated from the measured density profiles (see Appendix D). The quantitative prediction of our model (without any adjustable parameter) correctly reproduces the observed non-linear dependency of f_{coh} with f_c . We thus conclude that the heuristic model we introduced quantitatively captures the observed deviations to $g^{(n)}(0) = 1$ at $\mathbf{k} = \mathbf{0}$, attributing the latter to the presence of depleted atoms. In turns, this suggests that atoms in the BEC have the statistics of a fully coherent state, with $g^{(n)}(0) = 1$ at any order $n \leq 6$.

Note that in their evaluation of $g^{(3)}(0)$ in a BEC [30],

Hodgman *et al.* do not observe the small deviation reported here. A major difference with our experiment is that their observation volume V_Ω is quite large, as illustrated by the fact that in the thermal case it entails a convolution reducing the expected values of $g^{(2)}(0)$ or $g^{(3)}(0)$ from 2 and 6 to 1.022(2) and 1.061(6), respectively. We conclude that our ability to obtain good statistics in tiny volumes is a major asset of our experimental device.

V. CONCLUSION

We have presented measurements of the full counting statistics (FCS) and of perfectly-contrasted n -body correlations in interacting lattice Bose gases. We have investigated two iconic states of interacting lattice bosons, Mott insulators and lattice superfluids. We find that a Mott insulator exhibits a thermal statistics in the momentum space with $g^{(n)}(0) = n!$, while the condensate component is fully coherent with $g^{(n)}(0) = 1$ (at least) up to $n = 6$. The latter conclusion derives from assuming that the heuristic model we introduce to analyse the FCS in Bose superfluids and to describe the contribution from the depletion of the condensate is valid. We have assessed this validity from studying the coherent fraction at increasing interaction strengths. The results of this work represent the most stringent certifications of the many-body coherence properties of Mott insulators and of BECs, and they validate emblematic pure-state descriptions of n -body coherence up to the order $n = 6$.

In the future, the experimental approach we use is readily extendable to probe the many-body coherence in a large variety of interacting quantum states and phase transitions realized on cold-atom platforms (*e.g.* [9–11, 48]). It relies on (i) a free-fall expansion from the trap and (ii) a single-atom-resolved detection method. The first condition is ensured with lattice or low-dimensional (1D and 2D) gases for which interactions do not affect the expansion, as well as with quantum gases for which interactions are switched off during the expansion [49]. The second condition is met with various detection methods and atomic species [50].

Another interesting direction consists in realizing recent proposals to access non-trivial n -body correlations [23, 24]. These theoretical works have shown that non-diagonal correlators can be accessed from combining two-particle unitary transformations – *e.g.* beamsplitters – with a measurement of the FCS. Such protocols have many potential applications, from quantifying entanglement to implementing variational algorithms.

ACKNOWLEDGEMENT

We thank S. Butera, A. Browaeys, I. Carusotto, T. Lahaye, T. Roscilde and the members of the Quantum

Gas group at Institut d'Optique for insightful discussions. We acknowledge financial support from the Région Ile-de-France in the framework of the DIM SIRTEQ, the “Fondation d’entreprise iXcore pour la Recherche”, the Agence Nationale pour la Recherche (Grant num-

ber ANR-17-CE30-0020-01). D.C. acknowledges support from the Institut Universitaire de France. A. A. acknowledges support from the Simons Foundation and from Nokia-Bell labs.

-
- [1] Blanter, Y. and Büttiker, M., *Shot noise in mesoscopic conductors*, **Physics Reports** **336**, 1 (2000).
 - [2] Gardiner, C. and Zoller, P., *Quantum Noise - A Handbook of Markovian and Non-Markovian Quantum Stochastic Methods with Applications to Quantum Optics* (Springer Berlin, Heidelberg, 2004).
 - [3] Burt, E. A., Ghrist, R. W., Myatt, C. J., Holland, M. J., Cornell, E. A. and Wieman, C. E., *Coherence, Correlations, and Collisions: What One Learns about Bose-Einstein Condensates from Their Decay*, **Phys. Rev. Lett.** **79**, 337 (1997).
 - [4] Altman, E., Demler, E. and Lukin, M. D., *Probing many-body states of ultracold atoms via noise correlations*, **Phys. Rev. A** **70**, 013603 (2004).
 - [5] Schweigler, T., Kasper, V., Erne, S., Mazets, I., Rauer, B., Cataldini, F., Langen, T., Gasenzer, T., Berges, J. and Schmiedmayer, J., *Experimental characterization of a quantum many-body system via higher-order correlations*, **Nature** **545**, 323 (2017).
 - [6] Levitov, L. S., Lee, H. and Lesovik, G. B., *Electron counting statistics and coherent states of electric current*, **Journal of Mathematical Physics** **37**, 4845 (1996).
 - [7] Ivanov, D. A. and Abanov, A. G., *Phase transitions in full counting statistics for periodic pumping*, **EPL (Europhysics Letters)** **92**, 37008 (2010).
 - [8] Gómez-Ruiz, F. J., Mayo, J. J. and del Campo, A., *Full Counting Statistics of Topological Defects after Crossing a Phase Transition*, **Phys. Rev. Lett.** **124**, 240602 (2020).
 - [9] Devillard, P., Chevallier, D., Vignolo, P. and Albert, M., *Full counting statistics of the momentum occupation numbers of the Tonks-Girardeau gas*, **Phys. Rev. A** **101**, 063604 (2020).
 - [10] Eisler, V., *Universality in the Full Counting Statistics of Trapped Fermions*, **Phys. Rev. Lett.** **111**, 080402 (2013).
 - [11] Lovas, I., Dóra, B., Demler, E. and Zaránd, G., *Full counting statistics of time-of-flight images*, **Phys. Rev. A** **95**, 053621 (2017).
 - [12] Klich, I. and Levitov, L., *Quantum Noise as an Entanglement Meter*, **Phys. Rev. Lett.** **102**, 100502 (2009).
 - [13] Esposito, M., Harbola, U. and Mukamel, S., *Nonequilibrium fluctuations, fluctuation theorems, and counting statistics in quantum systems*, **Rev. Mod. Phys.** **81**, 1665 (2009).
 - [14] Gustavsson, S., Leturcq, R., Simović, B., Schleser, R., Ihn, T., Studerus, P., Ensslin, K., Driscoll, D. C. and Gossard, A. C., *Counting Statistics of Single Electron Transport in a Quantum Dot*, **Phys. Rev. Lett.** **96**, 076605 (2006).
 - [15] Maisi, V. F., Kambly, D., Flindt, C. and Pekola, J. P., *Full Counting Statistics of Andreev Tunneling*, **Phys. Rev. Lett.** **112**, 036801 (2014).
 - [16] Liebisch, T. C., Reinhard, A., Berman, P. R. and Raithel, G., *Atom Counting Statistics in Ensembles of Interacting Rydberg Atoms*, **Phys. Rev. Lett.** **95**, 253002 (2005).
 - [17] Malossi, N., Valado, M. M., Scotto, S., Huillery, P., Pillet, P., Ciampini, D., Arimondo, E. and Morsch, O., *Full Counting Statistics and Phase Diagram of a Dissipative Rydberg Gas*, **Phys. Rev. Lett.** **113**, 023006 (2014).
 - [18] Zeiher, J., van Bijnen, R., Schauß, P., Hild, S., Choi, J.-y., Pohl, T., Bloch, I. and Gross, C., *Many-body interferometry of a Rydberg-dressed spin lattice*, **Nature Physics** **12**, 1095 (2016).
 - [19] Öttl, A., Ritter, S., Köhl, M. and Esslinger, T., *Correlations and Counting Statistics of an Atom Laser*, **Phys. Rev. Lett.** **95**, 090404 (2005).
 - [20] Perrier, M., Amodjee, Z., Dussarrat, P., Dareau, A., Aspect, A., Cheneau, M., Boiron, D. and Westbrook, C. I., *Thermal counting statistics in an atomic two-mode squeezed vacuum state*, **SciPost Phys.** **7**, 2 (2019).
 - [21] Flammia, S. T., Gross, D., Liu, Y.-K. and Eisert, J., *Quantum tomography via compressed sensing: error bounds, sample complexity and efficient estimators*, **New Journal of Physics** **14**, 095022 (2012).
 - [22] Glauber, R. J., *The Quantum Theory of Optical Coherence*, **Phys. Rev.** **130**, 2529 (1963).
 - [23] Brunner, E., Buchleitner, A. and Dufour, G., *Many-body coherence and entanglement from randomized correlation measurements*, **arXiv** (2021), 10.48550/arxiv.2107.01686.
 - [24] Naldesi, P., Elben, A., Minguzzi, A., Clément, D., Zoller, P. and Vermersch, B., *Fermionic correlation functions from randomized measurements in programmable atomic quantum devices*, **arXiv** (2022), 10.48550/arxiv.2205.00981.
 - [25] Aspect, A., *Hanbury Brown and Twiss, Hong Ou and Mandel effects and other landmarks in quantum optics: from photons to atoms*, in **Current Trends in Atomic Physics**, edited by Browaeys, A., Lahaye, T., Porto, T., Adams, C. S., Weidemüller, M. and Cugliandolo, L. F. (Oxford University Press, 2019).
 - [26] Schellekens, M., Hoppeler, R., Perrin, A., Gomes, J. V., Boiron, D., Aspect, A. and Westbrook, C. I., *Hanbury Brown Twiss Effect for Ultracold Quantum Gases*, **Science** **310**, 648 (2005).
 - [27] Dall, R. G., Manning, A. G., Hodgman, S. S., RuGway, W., Kheruntsyan, K. V. and Truscott, A. G., *Ideal n-body correlations with massive particles*, **Nature Physics** **9**, 341 (2013).
 - [28] Jelte, T. et al., *Comparison of the Hanbury Brown-Twiss effect for bosons and fermions*, **Nature** **445**, 402 (2007).
 - [29] Bergschneider, A., Klinkhamer, V. M., Becher, J. H., Klemt, R., Palm, L., Zürn, G., Jochim, S. and Preiss, P. M., *Experimental characterization of two-particle entanglement through position and momentum correlations*, **Nature Physics** **15**, 640 (2019).
 - [30] Hodgman, S. S., Dall, R. G., Manning, A. G., Baldwin, K. G. H. and Truscott, A. G., *Direct Measurement of Long-Range Third-Order Coherence in Bose-Einstein*

- Condensates, *Science* **331**, 1046 (2011).
- [31] Carcy, C., Cayla, H., Tenart, A., Aspect, A., Mancini, M. and Clément, D., *Momentum-Space Atom Correlations in a Mott Insulator*, *Phys. Rev. X* **9**, 041028 (2019).
- [32] Cayla, H., Butera, S., Carcy, C., Tenart, A., Hercé, G., Mancini, M., Aspect, A., Carusotto, I. and Clément, D., *Hanbury Brown and Twiss Bunching of Phonons and of the Quantum Depletion in an Interacting Bose Gas*, *Phys. Rev. Lett.* **125**, 165301 (2020).
- [33] Tenart, A., Hercé, G., Bureik, J.-P., Dareau, A. and Clément, D., *Observation of pairs of atoms at opposite momenta in an equilibrium interacting Bose gas*, *Nature Physics* **17**, 1364 (2021).
- [34] Holten, M., Bayha, L., Subramanian, K., Brandstetter, S., Heintze, C., Lunt, P., Preiss, P. M. and Jochim, S., *Observation of Cooper pairs in a mesoscopic two-dimensional Fermi gas*, *Nature* **606**, 287 (2022).
- [35] Pitaevskii, L. P. and Stringari, S., *Bose-Einstein Condensation* (Clarendon press, Oxford, 2004).
- [36] Fölling, S., Gerbier, F., Widera, A., Mandel, O., Gericke, T. and Bloch, I., *Spatial quantum noise interferometry in expanding ultracold atom clouds*, *Nature* **434**, 481 (2005).
- [37] Toth, E., Rey, A. M. and Blakie, P. B., *Theory of correlations between ultracold bosons released from an optical lattice*, *Phys. Rev. A* **78**, 013627 (2008).
- [38] Walls, D. F. and Milburn, G. J., *Quantum Optics* (Springer Berlin, Heidelberg, 2008).
- [39] Kristensen, M. A., Christensen, M. B., Gajdacz, M., Iglicki, M., Pawłowski, K., Klempt, C., Sherson, J. F., Rzażewski, K., Hilliard, A. J. and Arlt, J. J., *Observation of Atom Number Fluctuations in a Bose-Einstein Condensate*, *Phys. Rev. Lett.* **122**, 163601 (2019).
- [40] Castin, Y. and Dum, R., *Low-temperature Bose-Einstein condensates in time-dependent traps: Beyond the U(1) symmetry-breaking approach*, *Phys. Rev. A* **57**, 3008 (1998).
- [41] Note that in the experiment the total atom number N is not strictly constant from shot to shot. However, the measurement of the FCS in a tiny volume V_Ω is largely immune to small shot-to-shot fluctuations of N .
- [42] Stenger, J., Inouye, S., Chikkatur, A. P., Stamper-Kurn, D. M., Pritchard, D. E. and Ketterle, W., *Bragg Spectroscopy of a Bose-Einstein Condensate*, *Phys. Rev. Lett.* **82**, 4569 (1999).
- [43] Cayla, H., Carcy, C., Bouton, Q., Chang, R., Carleo, G., Mancini, M. and Clément, D., *Single-atom-resolved probing of lattice gases in momentum space*, *Phys. Rev. A* **97**, 061609 (2018).
- [44] Tenart, A., Carcy, C., Cayla, H., Bourdel, T., Mancini, M. and Clément, D., *Two-body collisions in the time-of-flight dynamics of lattice Bose superfluids*, *Phys. Rev. Research* **2**, 013017 (2020).
- [45] Carcy, C., Hercé, G., Tenart, A., Roscilde, T. and Clément, D., *Certifying the Adiabatic Preparation of Ultracold Lattice Bosons in the Vicinity of the Mott Transition*, *Phys. Rev. Lett.* **126**, 045301 (2021).
- [46] Laiho, K., Dirmeier, T., Schmidt, M., Reitzenstein, S. and Marquardt, C., *Measuring higher-order photon correlations of faint quantum light: A short review*, *Physics Letters A* **435**, 128059 (2022).
- [47] Goodman, J. W., *Statistical optics*, edited by New York, W.-I., Vol. 1 (1985).
- [48] Contessi, D., Recati, A. and Rizzi, M., *Phase Diagram Detection via Gaussian Fitting of Number Probability*

Distribution, *arXiv*, 2207.01478 (2022).

- [49] Bloch, I., Dalibard, J. and Zwerger, W., *Many-body physics with ultracold gases*, *Rev. Mod. Phys.* **80**, 885 (2008).
- [50] Ott, H., *Single atom detection in ultracold quantum gases: a review of current progress*, *Reports on Progress in Physics* **79**, 054401 (2016).

Appendix A. DATA ANALYSIS OF CORRELATIONS IN MOTT INSULATORS

The Mott insulator is spread over the entire Brillouin zone in the momentum space, with a small density. As a consequence, the number of atoms falling in voxels of tiny volumes is small. In particular, the statistics of the atom number in a voxel smaller than the coherence volume is not sufficient to extract the magnitude $g^{(n)}(0)$ of the n -body correlation functions. To circumvent this issue, we proceed as follows.

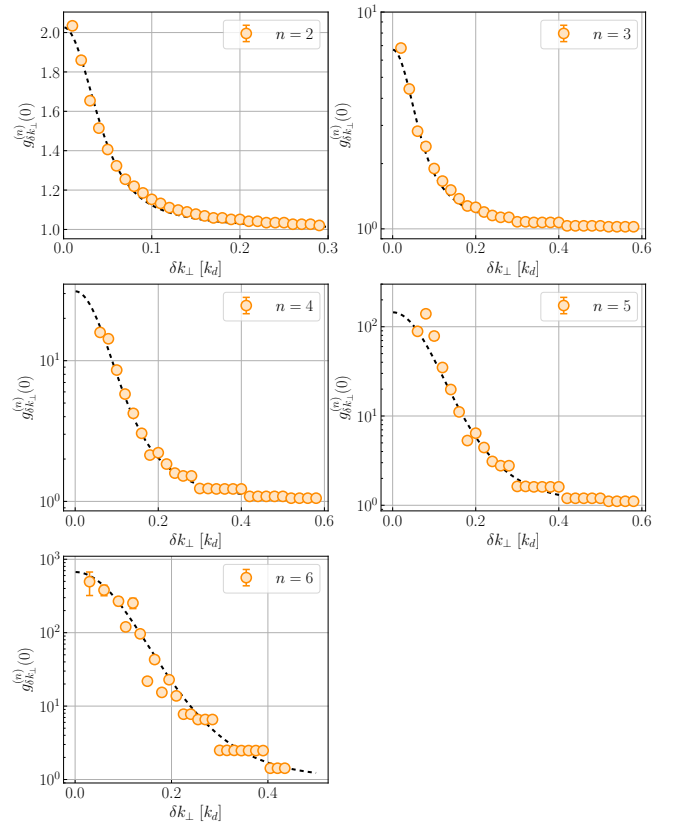


FIG. 5. Plot of the magnitude $g_{\delta k_{\perp}}^{(n)}(0)$ as a function of the transverse integration δk_{\perp} . The different panels correspond to different orders n of correlation functions, from $n = 2$ to $n = 6$. Apart from the data for $n = 2$ plotted in linear scale, the vertical axes are in log scale.

We first consider anisotropic voxels of volume $V(\delta k_{\perp}) = \delta k \times \delta k_{\perp}^2$ with $\delta k_{\perp} > l_c \gg \delta k$. The transverse integration over δk_{\perp} raises the statistics of the detected atom number $N_{\delta k_{\perp}}$, allowing us to compute the

factorial moments of $N_{\delta k_\perp}$ in each voxel labeled by the index j , $\langle N_{\delta k_\perp}(N_{\delta k_\perp} - 1) \dots (N_{\delta k_\perp} - n + 1) \rangle_j$. To further raise the statistics, we average the factorial moments over many such voxels, $\sum_j \langle N_{\delta k_\perp}(N_{\delta k_\perp} - 1) \dots (N_{\delta k_\perp} - n + 1) \rangle_j$ where \sum_j refers to the sum over all the voxels belonging to the first Brillouin zone.

The normalized correlation function $g_{\delta k_\perp}^{(n)}(\delta k)$ in voxels of volume $V(\delta k_\perp)$ is obtained from normalizing the factorial moments,

$$g_{\delta k_\perp}^{(n)}(\delta k) = \frac{\sum_j \langle N_{\delta k_\perp}(N_{\delta k_\perp} - 1) \dots (N_{\delta k_\perp} - n + 1) \rangle_j}{\sum_j \langle N_{\delta k_\perp} \rangle_j^n} \quad (5)$$

We then proceed by fitting the dependency of $g_{\delta k_\perp}^{(n)}(\delta k)$ with δk with a Gaussian function, from which we extract its magnitude $g_{\delta k_\perp}^{(n)}(0)$ at the considered transverse integration δk_\perp . At large transverse integrations, $\delta k_\perp \gg l_c$, $g_{\delta k_\perp}^{(n)}(0)$ is reduced with respect to the value $g^{(n)}(0)$ expected at vanishingly small integration, $\delta k_\perp \rightarrow 0$. To obtain $g^{(n)}(0)$, we repeat the calculation of $g_{\delta k_\perp}^{(n)}(0)$ for many values of δk_\perp , with the results shown in Fig. 5. From the plots in Fig. 5, we extrapolate the value $g^{(n)}(0)$ at $\delta k_\perp \rightarrow 0$.

Appendix B. DATA ANALYSIS OF CORRELATIONS IN BOSE SUPERFLUIDS

The magnitudes of the normalized correlation functions are obtained from the factorial moments of the atom number N_Ω in the small volume V_Ω . The n -factorial moment is defined as $\langle (N_\Omega)_n \rangle = \langle N_\Omega(N_\Omega - 1) \dots (N_\Omega - n + 1) \rangle$ and $g^{(n)}(0)$ are expressed as

$$g^{(n)}(0) = \frac{\langle N_\Omega(N_\Omega - 1) \dots (N_\Omega - n + 1) \rangle}{\langle N_\Omega \rangle^n} = \frac{\langle (N_\Omega)_n \rangle}{\langle N_\Omega \rangle^n} \quad (6)$$

We define the error bars on $g^{(n)}(0)$ as $\Delta(N_\Omega)_n / \langle N_\Omega \rangle^n$, where $\Delta(N_\Omega)_n$ is the standard error of the factorial moment of order n ,

$$\Delta(N_\Omega)_n = \frac{1}{\sqrt{N_{\text{runs}}}} \sqrt{\langle (N_\Omega)_n^2 \rangle - \langle (N_\Omega)_n \rangle^2} \quad (7)$$

Appendix C. MODEL FOR THE ATOM NUMBER STATISTICS AT $\vec{k} = \vec{0}$ IN BOSE SUPERFLUIDS

We introduce a simple model to account for the presence of atoms belonging both to the BEC and to its depletion in the central voxel located at $\vec{k} = \vec{0}$. We assume that the statistical properties of the BEC mode are those of a coherent state, $g_{\text{BEC}}^{(n)}(0) = 1$. In contrast, the statistical properties of the depletion are assumed to be those of a thermal state, $g_{\text{dep}}^{(n)}(0) = n!$. This latter assumption holds because we consider a small voxel of

size $dk = 0.025k_d \ll l_c$ where the correlation length l_c is set by the inverse in-trap size $1/L$ of the gas (see the main text). Moreover, we further assume that the BEC and depletion operators are uncorrelated. This is valid because the voxel we consider is much smaller than the volume occupied by the depletion, implying that the correlation between the total number of BEC atoms and the total number of depleted atoms (in the canonical ensemble) can be safely neglected.

We are interested in the statistical properties of the atom number $\hat{N}_\Omega = a_\Omega^\dagger a_\Omega$ falling in the considered voxel, where $a_\Omega = a_{\text{BEC}} + a_{\text{dep}}$ is the sum of the operators associated with the BEC and the depletion. Since we assume the operators a_{BEC} and a_{dep} are uncorrelated, one simply obtains

$$\langle (a_\Omega^\dagger)^n a_\Omega^n \rangle = \sum_{p=1}^n \binom{n}{p}^2 \langle (a_{\text{BEC}}^\dagger)^p a_{\text{BEC}}^p (a_{\text{dep}}^\dagger)^{n-p} a_{\text{dep}}^{n-p} \rangle \quad (8)$$

where by definition $a_\Omega^n = \sum_{p=1}^n \binom{n}{p} a_{\text{BEC}}^p a_{\text{dep}}^{n-p}$. This leads to the formula given in the main text,

$$\begin{aligned} g^{(n)}(0) - 1 &= \frac{\langle (a_\Omega^\dagger)^n a_\Omega^n \rangle}{\langle a_\Omega^\dagger a_\Omega \rangle^n} - 1 \\ &= \sum_{p=1}^{n-1} \left[(n-p)! \binom{n}{p}^2 - \binom{n}{p} \right] f_{\text{coh}}^p (1 - f_{\text{coh}})^{n-p} \end{aligned}$$

Appendix D. RELATION f_{coh} VERSUS f_c .

The coherent fraction is approximatively given by

$$f_{\text{coh}} \simeq \frac{\rho_{\text{BEC}}(0)}{\rho_{\text{BEC}}(0) + \rho_{\text{dep}}(0)} \quad (9)$$

where $\rho_{\text{BEC}}(0)$ (*resp.* $\rho_{\text{dep}}(0)$) is the momentum density of the BEC (*resp.* of the depletion) at the center of the Brillouin zone, $\vec{k} = \vec{0}$. The condensate fraction is approximately given by

$$f_c \simeq \frac{\rho_{\text{BEC}}(0) \mathcal{V}_c}{\rho_{\text{BEC}}(0) \mathcal{V}_c + \rho_{\text{dep}}(0) \mathcal{V}_d} \quad (10)$$

where \mathcal{V}_c (*resp.* \mathcal{V}_d) is the total volume of the momentum-space occupied by the BEC (*resp.* by the depletion) normalized to the density at $\vec{k} = \vec{0}$. Combining these two definitions, one obtains the equation Eq. (4) of the main text.

To compare the prediction of Eq. (4) with the measurements, we need to evaluate the volumes \mathcal{V}_c and \mathcal{V}_d . We describe the BEC density profile with an isotropic function [42]

$$n_{\text{BEC}}(\mathbf{k}) = \rho_{\text{BEC}}(0) e^{-k^2/2\sigma_{\text{bec}}^2} \quad (11)$$

and the density profile of the depletion with a lorentzian function along each (uncoupled) lattice axis,

$$n_{\text{dep}}(\mathbf{k}) = \rho_{\text{dep}}(0) \prod_{j=x,y,z} \left(\frac{\sigma_{\text{dep}}^2/4}{k_j^2 + (\sigma_{\text{dep}}/2)^2} \right). \quad (12)$$

We obtain $\mathcal{V}_c = (\sqrt{2\pi}\sigma_{\text{bec}})^3$ and $\mathcal{V}_d = \left(\sigma_{\text{dep}} \arctan \left[\frac{k_d}{\sigma_{\text{dep}}} \right] \right)^3$. From fitting the measured density profiles with the above dependency, we obtain $\mathcal{V}_c/\mathcal{V}_d = 0.03(1)$, a value which we use to plot the theoretical prediction in Fig. 4.